Washington University School of Medicine
Digital Commons@Becker

2020-Current year OA Pubs | Open Access Publications

7-1-2023

Enhanced 3D visualization of human fallopian tube morphology using a miniature optical coherence tomography catheter

Hongbo Luo

Shuying Li

Sitai Kou

Yixiao Lin

Ian S Hagemann

See next page for additional authors

Follow this and additional works at: https://digitalcommons.wustl.edu/oa_4

 Part of the Medicine and Health Sciences Commons

Please let us know how this document benefits you.

Authors

Hongbo Luo, Shuying Li, Sitai Kou, Yixiao Lin, Ian S Hagemann, and Quing Zhu

Research Article Vol. 14, No. 7 / 1 Jul 2023 / Biomedical Optics Express 3225
Biomedical Optics EXPRESS

Enhanced 3D visualization of human fallopian tube morphology using a miniature optical coherence tomography catheter

HONGBO LUO,[1] SHUYING LI,[2] SITAI KOU,[2] YIXIAO LIN,[2] IAN S. HAGEMANN,[3,4] AND QUING ZHU[1,2,5,*]

[1]Department of Electrical & Systems Engineering, Washington University in St. Louis, St. Louis, MO 63130, USA
[2]Department of Biomedical Engineering, Washington University in St. Louis, St. Louis, MO 63130, USA
[3]Department of Pathology & Immunology, Washington University School of Medicine, St. Louis, MO 63130, USA
[4]Department of Obstetrics & Gynecology, Washington University School of Medicine, St. Louis, MO 63130, USA
[5]Department of Radiology, Washington University School of Medicine, St. Louis, MO 63110, USA
*zhu.q@wustl.edu

Abstract: We demonstrate the use of our miniature optical coherence tomography catheter to acquire three-dimensional human fallopian tube images. Images of the fallopian tube's tissue morphology, vasculature, and tissue heterogeneity distribution are enhanced by adaptive thresholding, masking, and intensity inverting, making it easier to differentiate malignant tissue from normal tissue. The results show that normal fallopian tubes tend to have rich vasculature accompanied by a patterned tissue scattering background, features that do not appear in malignant cases. This finding suggests that miniature OCT catheters may have great potential for fast optical biopsy of the fallopian tube.

© 2023 Optica Publishing Group under the terms of the Optica Open Access Publishing Agreement

1. Introduction

Ovarian cancer remains the deadliest of all gynecologic malignancies, and it is the fifth deadliest cancer among women in the United States [1]. Most ovarian cancers are diagnosed at stages III and IV, where the survival rate is only 25–30% [2]. Evidence now indicates a significant portion of high grade serous ovarian cancers arise from serous tubal intraepithelial carcinoma (STIC) in the fallopian tubes [3]. STIC may lead to high grade serous carcinoma of the ovary, the most lethal and prevalent type of ovarian cancer. Imaging the fallopian tube and detecting the disease early could significantly improve the survival of ovarian cancer patients. According to the literature [4], 85% of STICs are found in the fimbriated section of the fallopian tube, and 15% are found in the infundibulum. The ampulla and isthmus sections have relatively low incidences of STIC. Because STIC lesions measure only a few hundred microns, they can easily be missed during pathological evaluation, and current imaging modalities (e.g., ultrasound) are nowhere close to detecting lesions of these sizes.

Optical coherence tomography (OCT), with around 10-micron resolution, can reveal small lesions and structural changes in biological tissue. In recent years, OCT has been applied in identifying diseased ovaries and fallopian tubes [5–9]. Madore et al. [5] revealed the two-dimensional (2D) structure of the fallopian tube, performing pullback scanning of the lumen using a rigid fiber probe 10 cm long and 1.2 mm in diameter. They also compared en face OCT images of paraffin-embedded human fallopian tube specimens with histology. Keenan et al. [6] designed a miniaturized steerable falloposcope combing wide field imaging and OCT to detect malignancies in the epithelial lumen of fallopian tube. By pulling back the falloposcope with a linear motor, 2D OCT images can be formed. Other researchers have developed quantification methods to

#489708 https://doi.org/10.1364/BOE.489708
Journal © 2023 Received 16 Mar 2023; revised 10 May 2023; accepted 29 May 2023; published 12 Jun 2023

Biomedical Optics EXPRESS

differentiate malignant from normal and benign fallopian tubes. Kirillin et al. [7] differentiated normal and inflamed fallopian tubes using the signal intensity distribution difference. Zeng et al. [8] used an en face scattering coefficient map obtained from fitting A-lines based on Beer's law to differentiate cancerous from benign ovaries and benign fallopian tubes. Li et al. [9] calculated the pixel-wise attenuation coefficient map from A-lines to differentiate cancerous ovaries and fallopian tubes. Compared to ovarian tissue, where OCT B scans show quite a homogeneous scattering distribution, fallopian tube OCT B-scans reveal abundant irregular structures with low intensity regions buried inside highly scattering tissue. These low intensity regions may indicate vessels or fatty tissue, which have lower scattering coefficients and are connected in the three-dimensional (3D) volume. As is well-known, tumor vascular distribution depends on neo-angiogenesis. Analyzing the 3D distribution of these dim regions within OCT images of the fallopian tube may help us characterize fallopian tube malignancies. Histology, the gold standard for cancer diagnosis, has cell-level resolution; however, it can give us only the cross-sectional morphology. OCT, on the other hand, can provide 3D images within an ~ 1 mm depth range with useful resolution. Also, nearly no sample preparation is needed, which gives OCT the potential to be performed in vivo. However, in conventional OCT images, tissue with a high scattering coefficient is usually highlighted, making it difficult to visualize underlying tissue structures (e.g., vessels and fatty tissue) and their connectivity in the 3D volume. Although OCT angiography can extract vessel networks inside tissue, it is not sensitive to complex tumor angiogenesis, for example tumor ischemia. Also, OCT angiography requires an expensive fast-scanning light source and oversampled scanning.

Photoacoustic microscopy, which generates a high vasculature contrast inside tissue, is another method to characterize vessel networks inside tissue [10,11]. In recent years, researchers have applied OCT and photoacoustic microscopy for vascular and structural morphology analysis in various tissue types. Nandy et al. [12] implemented full-field OCT combined with five image histogram features (mean, variance, skewness, kurtosis, and entropy) to analyse the texture of ex vivo ovarian samples. Rao et al. [13] and Leng et al. [14] implemented benchtop photoacoustic microscopy to acquire vasculature information from ovary and fallopian tube ex vivo samples. Mean vessel diameter, vascular density, vascular directionality, vascular definition, tortuosity/branches, and PA signal variance were extracted to distinguish malignant from benign tissues. Other methods such as micro-CT and MRI have also been applied by researchers to image fallopian tube with a larger field of view. Castro et al. [15] studied the vasculature of entire ex vivo fallopian tubes using micro-CT. They found that normal tubal vasculature became proportionally denser toward the tube's distal end, i.e., the fimbriae. In the clinical setting, Ma et al. [16] proposed to differentiate primary tubal cancers from primary ovarian cancers by studying tubal morphology using MRI. They found that cancerous fallopian tubes have a more homogenous "sausage-like" appearance and typically involve fluid buildup. However, limited by the resolution of MRI, most of their proposed MRI features were qualitative.

In this paper, we extract fallopian tube tissue underlying structures from conventional OCT 3D images, using an intensity inverting method to better visualize the tissue morphology in 3D without loss of depth information or resolution. 3D OCT visualization of different fallopian tube sections is also demonstrated for the first time. Special attention is paid to the fimbriae and infundibulum, the sections of the fallopian tube where most malignancies originate.

2. Materials and methods

2.1. OCT catheter

We used an OCT catheter reported in our previous study [17] to scan from the outside of the fallopian tube. The catheter has a 3.8 mm outer diameter and is composed of several parts: a glass tube for shielding, a motor for reflector rotation (Faulhaber, 0308B), a rod mirror (Edmund Optics, 54-092) for ~ 90-degree laser deflection, and a gradient refractive index (GRIN) lens

Biomedical Optics EXPRESS

for focusing. A swept source laser generator (Santec, HSL-2100, 1300 nm, 20 kHz) is the laser source, with ~ 6 mW power in the sample arm, and data acquisition is realized by a balanced detector (Thorlabs, PDB450C) and a data acquisition card (AlazarTech, ATS9462). In air, the axial and lateral resolutions are 6 microns and ~ 7 microns, respectively. An *ex vivo* fallopian tube sample is shown in Fig. 1 (a), and the imaging regions from different sections of the tube are marked with colored rectangles. The OCT catheter is placed in direct contact with the tissue surface in the imaging region, and 3D scans are generated from the outside of the fallopian tube.

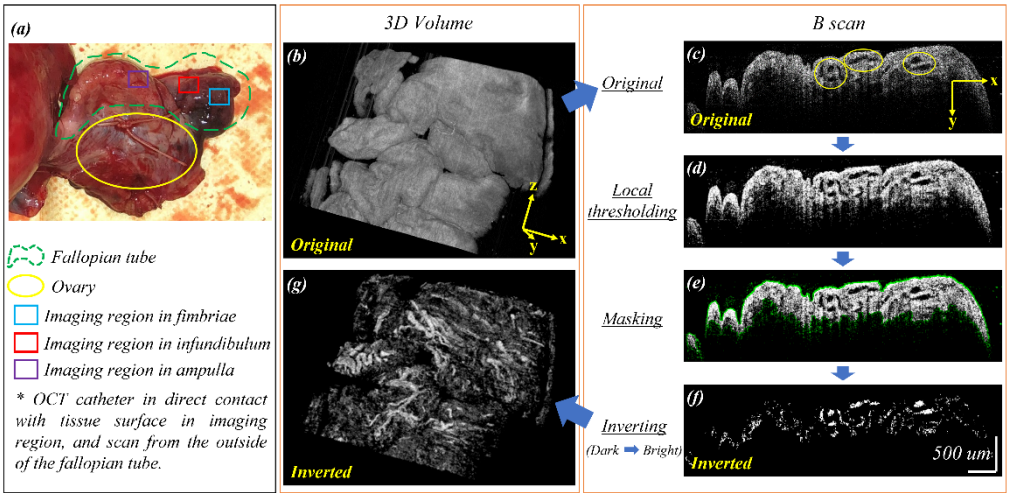

Fig. 1. (a). *Ex vivo* fallopian tube sample and 3D OCT scan locations. Figures 1 (b-g) Steps in generating intensity inverted 3D images: (b) An original 3D OCT image of a fallopian tube fimbriae section, displayed at a random angle with ImageJ 3Dviewer. (c) An original OCT B-scan image. (d) Adaptive thresholding applied to enhance contrast. (e) Masking applied to extract the signal region. (f) Signal intensity inverting applied. (g) 3D view of the intensity inverted image.

2.2. Fallopian tube specimens

Six freshly excised human fallopian tubes from 6 patients were imaged within 1 hour after surgery. For each specimen, one or more independent areas were scanned, resulting in a total of 8 independent areas among all 6 samples. After imaging, the specimens were returned to the Pathology Department for histological processing. The study protocol was approved by the local Institutional Review Boards and was HIPAA compliant. Informed consent was obtained from all patients.

2.3. 3D OCT image intensity inverting for structure extraction and visualization

To better see the underlying structures (e.g., vessels, fat) in fallopian tubes imaged with OCT, a 3D visualization tool based on adaptive thresholding and image intensity inverting was introduced. Figure 1 (b) shows an original 3D OCT image composed of 400 OCT B-scans displayed with ImageJ 3Dviewer [18,19]. The resolution of this 3D OCT volume is approximately 1600, 300, and 400 pixels in x, y, and z directions, covering an imaging volume of 10, 1.2, and 6 mm. Figure 1 (c) shows a single cross-sectional B-scan image from Fig. 1 (b). Various small low-intensity structures appear in the fallopian tube tissue, but the spatial distribution and connectivity of these structures are hard to visualize in 2D images.

Here, we tried to invert the 3D image to highlight the low intensity structures inside the tissue. The first step applies adaptive local thresholding binarization, using the Matlab function

Biomedical Optics EXPRESS

"adaptthres" to enhance image contrast. The purpose of using adaptive thresholding instead of a fixed threshold binarization is to preserve the dim regions with low contrast. The image after adaptive thresholding is shown in Fig. 1 (d). Next, a mask is generated to delimit the signal region before inverting: only the signal inside the masked region, not the low-intensity background, will be inverted in the next step. In Fig. 1 (e), the original signal is shown in green, and the masked interior region is depicted in black and white. The third step is to invert the signal, turning black into white and vice versa, as depicted in Fig. 1 (f). Note that only the signal in the masked region is inverted, and the signal outside of the masked region is set to zero as a dark background. Figure 1 (g) shows the 3D intensity inverted image with the ImageJ: this image can be rotated to any angle in the ImageJ software for better visualization. Compared to the original 3D OCT image in Fig. 1 (b), both vessel structures inside the tissue and the tissue heterogeneity are extracted and displayed in Fig. 1 (g).

3. Results

Four normal fallopian tubes were available from four patients. One malignant tube was available from a patient with surface and intramural deposits of carcinoma and another malignant tube was from a patient with metastatic high-grade carcinoma.

Figure 2 to Fig. 4 present original en face OCT images (left), intensity-inverted 3D images (middle-left), color-encoded depth images (middle-right) and H&E images (right), all from different sections of fallopian tubes. In the original en face OCT images in the left column, vessels and other low intensity structures are buried inside highly scattering tissue, obscuring their distribution inside the highly scattering background. In contrast, the middle column figures show 3D intensity inverted images. With the enhanced contrast generated by intensity inverting, the spatial distribution of vessels inside the tissue can be visualized clearly. With the help of the color-encoded depth images in the middle-right column, the different depths and connectivity of vessels inside the tissue can be further distinguished: red indicates a shallower depth, and blue represents a deeper region. Also, the intensity inverted 3D images can be rotated with ImageJ software for display at different angles.

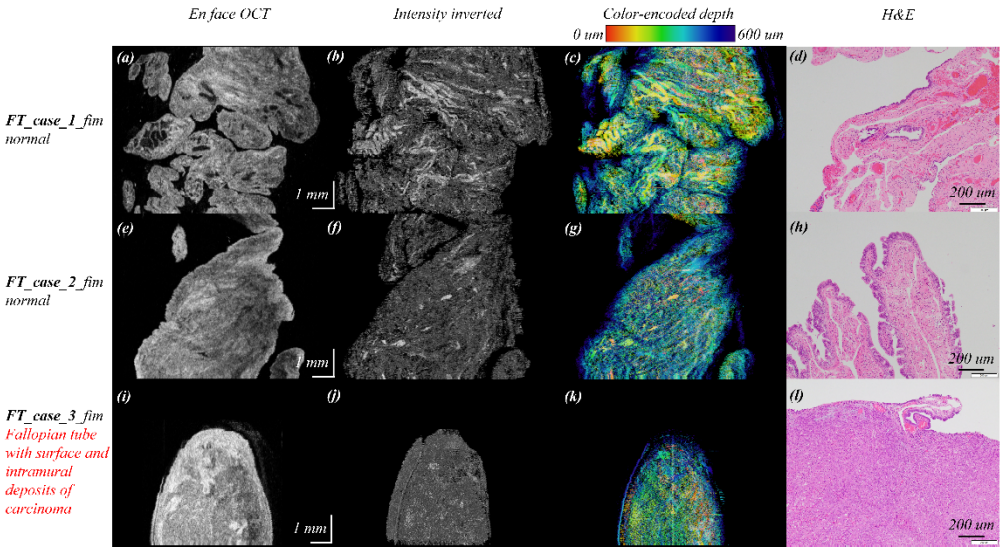

Fig. 2. 3D OCT scans from the fimbriae section.

Biomedical Optics EXPRESS

3.1. Fallopian tube – fimbriae

Figure 2 shows three images of the fimbriated section that we acquired from three different patients. Based on histology, one of these images, fallopian tube (FT) case_3, shows malignancy as shown in Fig. 2 (l), and the other two images (FT_case_1 and FT_case_2) are normal as depicted in Figs. 2 (d) and (h). The two normal cases are interesting and complex. Blood vessels, which are generally well visualized by OCT [20] and should presumably be uniformly present across normal tube specimens, have a variable propensity to appear in our images, which we hypothesize may be due to differences in the state of congestion during surgical procedures. For example, one case of fimbriae (FT_case_1) has very clear vessels (Fig. 2 (c)), while the other case (FT_case_2) lacks clear vessel features in both the OCT (Fig. 2 (g)) and H&E (Fig. 2 (h)) images, but has some background tissue heterogeneity showing striped patterns pointing towards the upper-right corner. This striped pattern might be generated by a uniformly arranged muscle layer or by mucosal folds extending from the fimbria. Both features, either abundant vessels or directionally patterned background tissue heterogeneity, can be used to characterize normal tissue in the fimbriated section. In the malignant case (FT_case_3), on the other hand, because of the surface and intramural deposits of carcinoma, few vessels can be seen in the intensity inverted 3D image (Fig. 2 (j)) and the H&E image (Fig. 2 (l)). Also, as depicted in the depth-color encoded image, the background tissue heterogeneity distribution is quite random, without any obviously organized pattern (Fig. 2 (k)).

3.2. Fallopian tube – infundibulum

Figure 3 shows four 3D images of the infundibulum of the fallopian tube that we acquired from three patients. One image (FT_case_6) is from a patient with malignancy in the infundibulum. For the normal cases (two from FT_case_4 and one from FT_case_5), in the left column en face figures (Figs. 3 (a) (e) (i)), we can see vessel cross sections in the shapes of dark stripes and dots buried inside the highly scattering tissue. The spatial distribution of these vessels is revealed in the intensity-inverted images in the middle column. In our observations of these fallopian images, the infundibulum section is generally rich in vessels, and the diameters and densities of vessels vary significantly among patients and among different infundibulum regions within a single patient.

Here, for the malignant case (FT_case_6) with metastatic high-grade carcinoma, unlike the three normal cases, the intensity inverted image (Fig. 3 (n)) in the middle shows tissue with discontinuous and irregular structures inside, instead of sharply defined and continuously connected vessel structures. Since the connectivity of the vessel is a 3D feature, this vessel connectivity difference is hard to see in cross-sectional images, e.g., en face and H&E, but it shows up clearly in 3D OCT intensity inverted images.

3.3. Fallopian tube – ampulla

Figure 4 shows one normal image from the ampulla of one tube. This normal case is rich in vessels, and these vessels appear deeper (bluer in the color-encoded depth image) than the structures in the infundibulum and the fimbriated sections.

In summary, different sections of the fallopian tube show different morphological features. In normal cases, the infundibulum and the fimbriated sections have the most shallow and organized vessel structures, while the ampulla section has deeper vessel structures. Organized uni-directional background tissue heterogeneity due to mucosal folds or muscle fibers is also one important feature in these regions. In malignant cases, the vessel structure and the uni-directional tissue heterogeneity pattern either disappear or are destroyed, replaced by randomly distributed background tissue heterogeneity or discontinuous and irregular structures.

Biomedical Optics EXPRESS

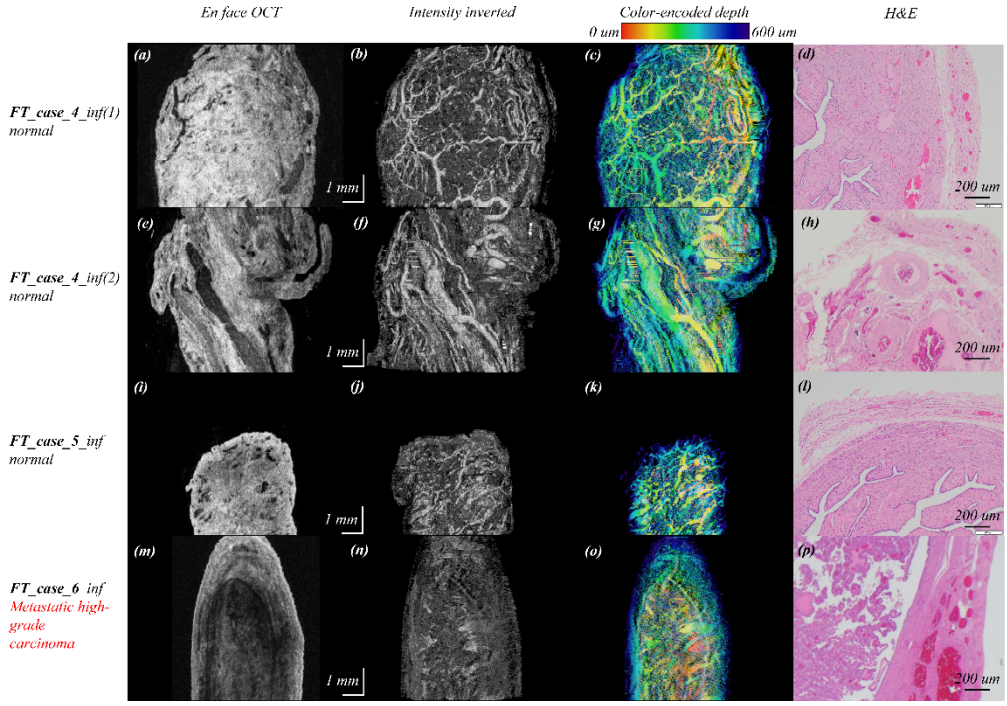

Fig. 3. 3D OCT scans from the infundibulum section.

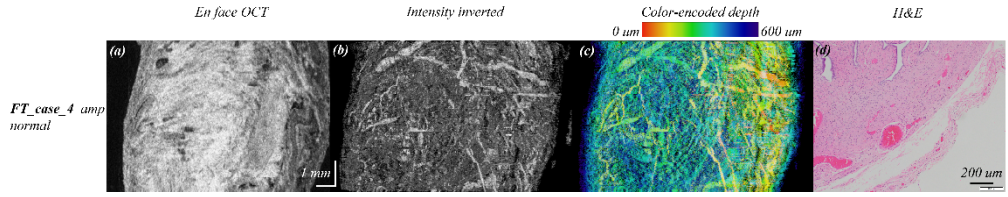

Fig. 4. One 3D OCT scan from the ampulla section.

3.4. Directionality analysis

To better characterize the intensity inverted images and differentiate normal from malignant cases, the ImageJ "Directionality" function can be exploited to analyze the vessel structures in the images. For each case, the analysis proceeds through five steps. (1) A max intensity projection is used on the 3D intensity inverted images to generate a 2D en face image. (2) A 5 by 5 median filter is used to reduce the image noise. (3) Images are cropped into smaller regions with a resolution of 150 by 150 (physical size around 900 μm by 1125 μm) for directionality analysis, and cropped images with strong boundaries and artefacts are removed. (4) Gaussian fitting within the "Directionality" function is used to determine if the image has a strong directionality. Finally, (5) the goodness of fit (based on R-square, with a value closer to 1 indicating a better fit) is used as a summary statistic for directionality of the image. The directionality of our fallopian tube cases is shown in Fig. 5.

Figure 5 (a) shows the result for the fimbriated section of the tube. For analysis, 22 cropped images from normal tubes and 6 cropped images from malignant tubes were used. As can be seen, the malignant case has significantly lower goodness of fit values, since neither vessels nor a

Biomedical Optics EXPRESS

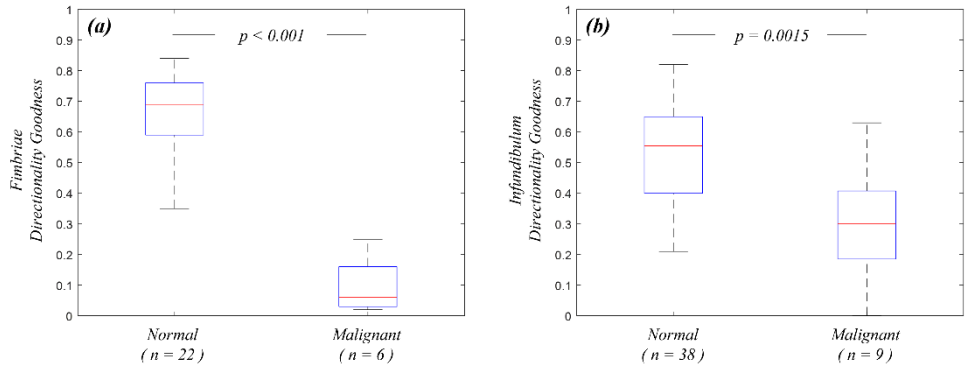

Fig. 5. Directionality analysis: (a) Fimbriated section, and (b) Infundibulum.

striped tissue heterogeneity background was observed in this case, as shown in the color-encoded depth image in Fig. 2.

Figure 5 (b) shows the result for the infundibulum section. For analysis, 38 cropped images from normal regions and 9 cropped images from the malignant region were used. Since vessels show up in this malignant case, as seen in the color-encoded depth image in Fig. 3, the goodness value range is large, and nearly half of the data set overlaps with the normal cases' range. However, several low goodness values below 0.2 are observed in the malignant case, which are not observed in any of the normal cases. These low goodness values are generated by the image regions of discontinuous and irregular structures with no strong directionality.

4. Discussion and conclusion

Although the intensity-inverted images can enhance the visualization of the low intensity region structures inside the fallopian tube, there are several drawbacks of this intensity based method. First, a common feature of the extracted structures is that they are dark in the original 3D OCT images, and several structures, such as fat and vessels, are extracted together. Second, vessels and the background tissue heterogeneity are intermixed, which blurs the image and makes quantitative analysis difficult. However, the differentiation between them relies on shape and connectivity, which can be discerned by human observers. In the future, pattern recognition machine learning algorithms could be useful in identifying blood vessel networks and predicting diagnoses. Third, malignancy in the fallopian tube is rare, so it is challenging to collect enough cases to fully understand the differences among malignancies and between normal and malignant tubes. Fourth, due to tissue distortion from fixing, slicing, and the lack of fiducial markers, our OCT images and histology slices are not exactly co-registered. We can only guarantee they are from the same section of the fallopian tube. However, this limitation does not affect OCT image processing and statistical analysis. Fifth, our algorithm is still not robust enough during the "masking" process, which will include some of the dark background in the selected signal region. After intensity inverting, the included dark background will become bright signal and generate a "streak-like" artefact pattern in the intensity-inverted map, as depicted in Fig. 3 "FT_case_4_inf (2)". This artifact can be avoided by improved mask processing in the future.

In this paper, OCT is used for the first time to reveal the 3D morphology of fallopian tubes from multiple patients. Also, to better visualize the 3D fallopian tube images, a method based on intensity inverting is introduced, which clarifies the fallopian tube vessel morphology and the difference in tissue heterogeneity between normal and malignant cases. The results show that normal fallopian tubes tend to have rich vasculature accompanied by a patterned tissue scattering background, features that do not appear in malignant areas. While each tube may

Biomedical Optics EXPRESS

show a range of vascular directionality when considering multiple regions, it appears that the least-directional area of a given tube may be useful in predicting malignancy. Compared to OCT angiography and photoacoustic imaging, our approach is well suited for imaging tissue with or without vasculature because tissue heterogeneity is extracted at the same time, and a regularly patterned tissue heterogeneity indicates a normal fallopian tube based on our observation. In the future, this OCT catheter can be utilized in surgical operations for fast optical biopsy of the fallopian tube surface to assist physicians in examining subsurface vasculature, especially the fimbriated section of the fallopian tube which is wide open at the end of the fallopian tube. It can be easily accessed with our 3.8 mm OD catheter from the outside (i.e., from the abdominal cavity) without passing the catheter through the entire fallopian tube. Currently, we are developing a 1.5 mm OD OCT catheter that can be inserted into the fallopian tube lumen to image malignancies of the inner layer (mucosa).

Funding. National Cancer Institute (RO1CA237664).

Acknowledgments. We thank our OBGYN surgeons and pathology fellows and residents for helping with specimen studies and Professor James Ballard for reviewing and editing the manuscript.

Disclosures. The authors declare no conflicts of interest.

Data availability. Associated code will be uploaded to [21]. Data is available from the corresponding author upon reasonable request.

References

1. R. L. Siegel, K. D. Miller, H. E. Fuchs, and A. Jemal, "Cancer statistics, 2022," CA A Cancer J Clinicians **72**(1), 7–33 (2022).
2. J. Jin, "Screening for Ovarian Cancer," JAMA - J. Am. Med. Assoc. **319**(6), 624 (2018).
3. J. Ducie, F. Dao, M. Considine, N. Olvera, P. A. Shaw, R. J. Kurman, I. M. Shih, R. A. Soslow, L. Cope, and D. A. Levine, "Molecular analysis of high-grade serous ovarian carcinoma with and without associated serous tubal intra-epithelial carcinoma," Nat. Commun. **8**(1), 990 (2017).
4. E. Schmoeckel, A. A. Odai-Afotey, M. Schleißheimer, M. Rottmann, A. Flesken-Nikitin, L. H. Ellenson, T. Kirchner, D. Mayr, and A. Y. Nikitin, "LEF1 is preferentially expressed in the tubal-peritoneal junctions and is a reliable marker of tubal intraepithelial lesions," Mod. Pathol. **30**(9), 1241–1250 (2017).
5. W. J. Madore, E. De Montigny, A. Deschênes, F. Benboujja, M. Leduc, A. M. Mes-Masson, D. M. Provencher, K. Rahimi, C. Boudoux, and N. Godbout, "Morphologic three-dimensional scanning of fallopian tubes to assist ovarian cancer diagnosis," J. Biomed. Opt **22**(7), 076012 (2017).
6. M. Keenan, T. H. Tate, K. Kieu, J. F. Black, U. Utzinger, and J. K. Barton, "Design and characterization of a combined OCT and wide field imaging falloposcope for ovarian cancer detection," Biomed. Opt. Express **8**(1), 124–136 (2017).
7. M. Kirillin, "Criteria for pathology recognition in optical coherence tomography of fallopian tubes," J. Biomed. Opt **17**(8), 081413 (2012).
8. Y. Zeng, S. Nandy, B. Rao, S. Li, A. R. Hagemann, L. K. Kuroki, C. McCourt, D. G. Mutch, M. A. Powell, I. S. Hagemann, and Q. Zhu, "Histogram analysis of en face scattering coefficient map predicts malignancy in human ovarian tissue," J. Biophotonics **12**(11), e201900115 (2019).
9. S. Li, H. Luo, S. Kou, I. S. Hagemann, and Q. Zhu, "Depth-resolved Attenuation Mapping of the Human Ovary and Fallopian Tube Using Optical Coherence Tomography," J. Biophotonics **12**, e202300002 (2023).
10. J. Laufer, P. Johnson, E. Zhang, B. Treeby, B. Cox, B. Pedley, and P. Beard, "In vivo preclinical photoacoustic imaging of tumor vasculature development and therapy," J. Biomed. Opt. **17**(5), 1–056016 (2012).
11. S. Hu and L. V. Wang, "Photoacoustic imaging and characterization of the microvasculature," J. Biomed. Opt. **15**(1), 011101 (2010).
12. S. Nandy, M. Sanders, and Q. Zhu, "Classification and analysis of human ovarian tissue using full field optical coherence tomography," Biomed. Opt. Express **7**(12), 5182–5187 (2016).
13. B. Rao, X. Leng, Y. Zeng, Y. Lin, R. Chen, Q. Zhou, A. R. Hagemann, L. M. Kuroki, C. K. McCourt, D. G. Mutch, and M. A. Powell, "Optical resolution photoacoustic microscopy of ovary and fallopian tube," Sci. Rep. **9**(1), 14306 (2019).
14. X. Leng, S. Kou, Y. Lin, A. R. Hagemann, I. S. Hagemann, P. H. Thaker, L. M. Kuroki, C. K. McCourt, D. G. Mutch, C. Siegel, and M. A. Powell, "Quantification of ovarian lesion and fallopian tube vasculature using optical-resolution photoacoustic microscopy," Sci. Rep. **12**(1), 15850 (2022).
15. P. T. Castro, O. L. Aranda, E. Marchiori, L. F. B. D. Araújo, H. D. L. Alves, R. T. Lopes, H. Werner, and E. Araujo Júnior, "Proportional vascularization along the fallopian tubes and ovarian fimbria: assessment by confocal microtomography," Radiol. Bras. **53**(3), 161–166 (2020).
16. F. H. Ma, S. Q. Cai, J. W. Qiang, S. H. Zhao, G. F. Zhang, and Y. M. and Rao, "MRI for differentiating primary fallopian tube carcinoma from epithelial ovarian cancer," J. Magn. Reson. Imaging **42**(1), 42–47 (2015).

Biomedical Optics EXPRESS

17. H. Luo, S. Li, Y. Zeng, H. Cheema, E. Otegbeye, S. Ahmed, W. C. Chapman Jr, M. Mutch, C. Zhou, and Q. Zhu, "Human colorectal cancer tissue assessment using optical coherence tomography catheter and deep learning," J. Biophotonics **15**(6), e202100349 (2022).
18. C. A. Schneider, W. S. Rasband, and K. W. Eliceiri, "NIH Image to ImageJ: 25 years of image analysis," Nat. Methods **9**(7), 671–675 (2012).
19. B. Schmid, J. Schindelin, A. Cardona, M. Longair, and M. Heisenberg, "A high-level 3D visualization API for Java and ImageJ," BMC Bioinf. **11**(1), 274 (2010).
20. J. Yang, S. Chang, I. A. Chen, S. Kura, G. A. Rosen, N. A. Saltiel, B. R. Huber, D. Varadarajan, Y. Balbastre, C. Magnain, and S. C. Chen, "Volumetric characterization of microvasculature in ex vivo human brain samples by serial sectioning optical coherence tomography," IEEE Trans. Biomed. Eng. **69**(12), 3645–3656 (2022).
21. H. Luo, S. Li, S. Kou, Y. Lin, I. S. Hagemann, and Q. Zhu, "Enhanced 3D visualization of human fallopian tube morphology using a miniature optical coherence tomography catheter: code," Github, 2022, https://github.com/OpticalUltrasoundImaging/OCT_intensity_reversal_code.

128.252.210.1 {ts '2023-08-07 12:17:17'}